Acta Pharmaceutica Sinica B 2024;14(1):405−420

Chinese Pharmaceutical Association
Institute of Materia Medica, Chinese Academy of Medical Sciences

Acta Pharmaceutica Sinica B

www.elsevier.com/locate/apsb
www.sciencedirect.com

ORIGINAL ARTICLE

The ERF transcription factor LTF1 activates DIR1 to control stereoselective synthesis of antiviral lignans and stress defense in *Isatis indigotica* roots

Ruibing Chen[a,g,†], Jian Yu[a,†], Luyao Yu[a,†], Liang Xiao[a,†], Ying Xiao[b], Junfeng Chen[b], Shouhong Gao[c], Xianghui Chen[d], Qing Li[c], Henan Zhang[e], Wansheng Chen[b,c,*], Lei Zhang[a,f,*]

[a]*Department of Pharmaceutical Botany, School of Pharmacy, Naval Medical University, Shanghai 200433, China*
[b]*Research and Development Center of Chinese Medicine Resources and Biotechnology, Shanghai University of Traditional Chinese Medicine, Shanghai 201203, China*
[c]*Department of Pharmacy, Shanghai Changzheng Hospital, Naval Medical University, Shanghai 200003, China*
[d]*School of Medicine, Shanghai University, Shanghai 200433, China*
[e]*Institute of Edible Fungi, Shanghai Academy of Agricultural Sciences, National Engineering Research Center of Edible Fungi, Key Laboratory of Edible Fungi Resources and Utilization (South), Ministry of Agriculture, Shanghai 201403, China*
[f]*College of Life Sciences and Medicine, Key Laboratory of Plant Secondary Metabolism and Regulation of Zhejiang Province, Zhejiang Sci-Tech University, Hangzhou 310018, China*
[g]*State Key Laboratory of Dao-di Herbs, Beijing 100700, China*

Received 1 June 2023; received in revised form 13 July 2023; accepted 7 August 2023

KEY WORDS

Lignans;
Stereoselective synthesis;
Stress resistance;
Dirigent protein;
ERF

Abstract Lignans are a powerful weapon for plants to resist stresses and have diverse bioactive functions to protect human health. Elucidating the mechanisms of stereoselective biosynthesis and response to stresses of lignans is important for the guidance of plant improvement. Here, we identified the complete pathway to stereoselectively synthesize antiviral (−)-lariciresinol glucosides in *Isatis indigotica* roots, which consists of three-step sequential stereoselective enzymes DIR1/2, PLR, and UGT71B2. DIR1 was further identified as the key gene in respoJanuary 2024nse to stresses and was able to trigger stress defenses by mediating the elevation in lignan content. Mechanistically, the phytohormone-responsive

*Corresponding authors.
E-mail addresses: chenws126@126.com (Wansheng Chen), starzhanglei@aliyun.com (Lei Zhang).
†These authors made equal contributions to this work.
Peer review under the responsibility of Chinese Pharmaceutical Association and Institute of Materia Medica, Chinese Academy of Medical Sciences.

https://doi.org/10.1016/j.apsb.2023.08.011

ERF transcription factor LTF1 colocalized with DIR1 in the cell periphery of the vascular regions in mature roots and helped resist biotic and abiotic stresses by directly regulating the expression of DIR1. These systematic results suggest that DIR1 as the first common step of the lignan pathway cooperates with PLR and UGT71B2 to stereoselectively synthesize (−)-lariciresinol derived antiviral lignans in *I. indigotica* roots and is also a part of the LTF1-mediated regulatory network to resist stresses. In conclusion, the LTF1-DIR1 module is an ideal engineering target to improve plant Defenses while increasing the content of valuable lignans in plants.

1. Introduction

The accumulation level of bioactive metabolites and the ability to resist stresses determine the quality of medicinal plants. Lignans are a large group of natural products derived from the oxidative coupling of two coniferyl alcohol molecules. Owing to the stress-resistant function and biological activities, lignans are important for plant growth and human health. Therefore, it is of great significance to elucidate the biosynthesis and regulation mechanism of lignans for the guidance of optimizing plants, whether to improve the stress resistance or the content of active lignans.

Plants are not motile and thus they must endure a variety of stresses, especially the root-based environmental stresses underground, such as high salinity and pathogen infection. Fortunately, plants have evolved powerful defense mechanisms in roots to withstand and adapt to their environments[1,2]. When environmental stress signals are sensed, plants can directly resist stresses by regulating the accumulation of secondary metabolites with the guidance of multistage signal transduction[3]. Plants produce a series of secondary metabolites to govern interactions with and adaptation to their biotic and abiotic environments[4−7]. Lignans are ubiquitously present in all plants that contain lignin (most land plants) and have long been considered as potential metabolites that increased tolerance to stress[8,9]. After the activity against insects of the lignans sesamin, asarin and pinoresinol was first proposed through *in vitro* tests in 1942[10], a series of stress-resistant lignans were discovered *in vitro*[11]. Western red cedar (*Thuja plicata*) accumulates relatively large amounts of lignans, which are derived from plicatic acid in the heartwood, as part of a complex system that may increase pest and disease resistance[12,13]. Pinoresinol, as one of the simplest lignans, is synthesized from two molecules of coniferyl alcohol through 8−8′ radical coupling reactions and has antihelminthic and antifungal activities *in vitro*[14,15]. Our previous study found that the synthesis and accumulation of pinoresinol and its derivatives were regulated by methyl jasmonate (MeJA) in *Isatis indigotica*, suggesting its potential involvement in the response to stresses[16,17]. However, the actual stress-resistant potential *in vivo* and the application potentiality to increase plant tolerance of lignans remains to be confirmed.

Lignans have also received wide attention as leading compounds of novel drugs for the treatment of tumor and virus infection, as well as healthy diets to reduce the risks of lifestyle-related non-communicable diseases[8,18,19]. Sesamin and its metabolites exhibited anti-hypertensive, anticancer, immunomodulatory, and anti-inflammatory activities[20−22]. It is worth noting that the activities of most lignans are closely related to the stereo configuration of lignans. The (−)-podophyllotoxin (isolated from *Podophyllum* plants) and its semi-synthetic derivatives, (−)-etoposide, (−)-teniposide, and (−)-etopophos, are clinically utilized to treat testicular and small-cell lung cancer[23]. (−)-gossypol, instead of (+)-gossypol, is the bioactive form with anti-spermatogenic activity in mammals[24]. These active lignans with specific stereo configurations are typically distributed in specific tissues at low content levels and are even accumulated only in some endangered plants, which hinders the efficient and stable production[25,26]. Therefore, understanding and exploiting the mechanisms of lignan stereoselective synthesis and regulation will prompt the discovery of rational intervention strategies toward desired plant improvement for higher lignan content and stronger plant defense.

The biosynthetic pathways of lignans and flavonoids share the upstream of shikimate and phenylpropanoid pathways to produce phenolic acids that are further converted to the lignan precursor coniferyl alcohol (Supporting Information Fig. S1). In this process, chorismic acid is first converted to L-phenylalanine, which is used to synthesize cinnamic acid by phenylalanine ammonia-lyase (PAL). Cinnamic acid is then hydroxylated by a cytochrome P450 monooxygenase (CYP) cinnamate 4-hydroxylase (C4H) to form *p*-coumaric acid. Furthermore, the sequential reactions catalyzed by 4CL (4-(hydroxy) cinnamoyl CoA ligase), CCoAOMT (caffeoyl CoA *O*-methyltransferase), CCR (cinnamoyl CoA reductase), and CAD (cinnamyl alcohol dehydrogenase) achieve the biosynthesis of coniferyl alcohol. The pathway of all lignans in plants is started from a common first step, the electron coupling reaction of coniferyl alcohol to produce the key lignan molecule pinoresinol with stereo configuration, which is accomplished by Dirigent (DIR) protein, followed by the production of diverse lignan structures through specific downstream enzymes, such as pinoresinol-lariciresinol reductase (PLR), CYP, and UDP-glucotransferase (UGT), etc.[27−31]. DIR as the first step of the lignan pathway mediates the regio- and stereoselectivity of bimolecular phenoxy radical coupling reactions for (−)-pinoresinol[32] or (+)-pinoresinol[33] biosynthesis, which preliminarily determines the stereo configuration of lignans in a plant. In addition, DIRs are also involved in the formation of Casparian strips in roots[34] and the atroposelective synthesis of gossypol[24,35,36]. Lignan synthesis is very sensitive to environmental changes[31,37−39]. Although several stress- and phytohormone-responsive transcript factors have been identified to explain the susceptible perturbation of lignan biosynthesis, these affect all are indirectly mediated through upstream genes of phenylpropanoid and aromatic alcohol pathway (phenylalanine ammonia-lyase, PAL; coumarate3-hydroxylase, C3H; 4-coumarate: CoA ligase, 4CL; cinnamoyl-CoA reductase,

CCR) rather than the actual lignan pathway[40,41], which suggests that the effect of these transcription factors on lignan synthesis is probably a side effect, and the actual regulatory target is the stress-resistant flavonoids and lignin. Therefore, the transcription factor that directly regulates lignan synthesis has not been discovered so far, that is, the specific regulatory mechanism of lignan response and adaptation to environmental stress is still unclear.

The root of *I. indigotica* (Radix Isatidis), with the Chinese name "Ban Lan Gen", is frequently used for the treatment of influenza and hepatitis because of antiviral lariciresinol glucosides[25,26,42] and indole alkaloids[43], as well as their derivatives. Therefore, this study aims to elucidate the stereoselective synthesis and the response mechanism to stresses of antiviral lariciresinol glucosides in *I. indigotica,* which can guide the improvement of the herbal quality of Radix isatidis. Here, we found that the (−)-lariciresinol glucosides are the primary antiviral components in *I. indigotica* roots, which are synthesized through continuous stereoselective reactions catalyzed by DIR1/2, PLR, and UGT71B2. Two of the 19 DIRs (DIR1 and DIR2) were identified in *I. indigotica* roots mediating the regio- and stereoselective synthesis of (−)-pinoresinol, which is further converted to (−)-lariciresinol and (+)-secoisolariciresinol by lariciresinol glucosides by UGT71B2, although UGT71B2 prefers to react with (+)-lariciresinol. Constitutive overexpression of DIR1 and DIR2 in hairy roots significantly increased lignan and lignin biosynthesis because of their regioselectivity; furthermore, overexpression enhanced the hairy root resistance to biotic and abiotic stresses, which suggested the definite stress-resistant function of lignans *in vivo*. Despite having redundant biochemical functions, the expression patterns of DIR1 and DIR2 are completely different. DIR1 is specifically localized in the cell periphery of vascular regions in mature roots and is regulated by a variety of phytohormones synergistically or antagonistically. Furthermore, we identified an ERF transcriptional regulator LTF1 that regulates lignan biosynthesis through DIR expression in response to abiotic and biotic stresses. LTF1 is the first transcription factor found to directly and specifically regulate the lignan pathway, and its regulatory target DIR is the first common step for the lignan synthesis in plants and the decisive step for lignan configuration. Lignans are ubiquitously present in all plants that contain lignin, and this study provides evidence of a novel mechanism by which the plant ERF-DIR module regulates lignan synthesis in response to stresses. In particular, the ERF-DIR module will be an ideal engineering target for enhancing plant stress resistance while increasing the content of valuable lignans, such as antiviral lignans in *I. indigotica*.

2. Materials and methods

2.1. Plant material and growth conditions

Flowers, leaves, stems, petioles, and roots were collected from 8-month-old plants. To collect sterilized seedlings, seeds of *I. indigotica* were surface sterilized in 75% ethanol for 1 min and then in sodium hypochlorite solution with 1.7% active chlorine for 15 min. After rinsing thoroughly five times with sterile distilled water, the seeds were placed on Murashige and Skoog (MS) medium (PhytoTech, USA) with 3% sucrose and 0.5% agar (pH 6.0).

2.2. sgRNA design and CRISPR/Cas9 vector construction

LTF1 was selected as the target locus for editing, and the sgRNA was designed by an online web tool (http://crispr.mit.edu/). Two potential 20-bp sequences followed by PAM from the ORF of LTF1 (no introns of the LTF1 DNA sequence) were used for the CRISPR/Cas9-mediated efficient targeted mutagenesis of LTF1 according to published protocols[44,45].

2.3. Construction of plant overexpression vectors

To create overexpression hairy roots, the coding sequences of DIR1, DIR2, and LTF1 were separately cloned into the *p*HB-X-myc vector with *Bam*H I and *Sac* I restriction sites. The empty vector *p*HB-X-myc was used as the control without exogenous gene insertion into the vector.

2.4. Plant transformation of hairy roots

The transgenic hairy roots were cultured through the induction of *Agrobacterium rhizogenes* C58C1 harboring the proper plasmids as described by reference[39]. The hairy roots were weighed each week and harvested after 9 weeks for DNA extraction, RNA extraction, metabolite determination, microscopic analysis, phloroglucinol-HCl staining, GUS staining, and induction assays according to corresponding protocols.

2.5. Bioinformatics analysis

Phylogenetic analysis was performed using the neighbor-joining method with the pairwise deletion option in MEGA 5.05. The *cis*-elements of promoters were predicted using the PANTCARE tool (http://bioinformatics.psb.ugent.be/webtools/plantcare/html).

2.6. Protein heterologous expression

The coding sequences of DIRs were separately constructed into *p*PICZα for protein expression in *Pichia pastoris*. The expression process was performed according to the reference. The day after, the sample was subjected to a nickel-nitrilotriacetic acid (Ni-NTA) agarose affinity column for further purification[46].

The *p*ET28a vector was transformed into *Escherichia coli* BL21 (DE3) for the expression of LTF1, PLR, and UGT71B2. The expression was induced with 0.5 mmol/L IPTG followed by continued growth at 16 °C and 110 rpm for 16 h. The protein was extracted by sonication and purified by a Ni-NTA agarose affinity column for EMSAs.

2.7. Catalytic assays

In a total reaction mixture volume of 250 μL, a final concentration of 400 mmol/L MES (pH 6.0), 0.5 U/mL laccase (Sigma, product number 40452), and 1 mg/mL coniferyl alcohol was maintained along with purified DIR enzymes. The reaction mixture without DIRs served as a control. The reaction mixture was incubated at 30 °C and 500 rpm for 4 h and then quenched by adding 500 μL of ethyl acetate. Finally, the mixture was centrifuged to remove proteins and filtered through a 0.22 μm filter prior to analysis by high-performance liquid chromatography−tandem mass spectrometry (HPLC−MS−MS). The assays of enzyme activity for PLR and UGT71B2 were performed as previous methods [27,47].

2.8. Chemical extraction

Lignans were extracted from 500 mg of powdered lyophilized tissues. The samples were extracted two times in 15 mL methanol and sonicated for 10 min. Combined extracts were then centrifuged for 30 min at 4000 rpm, and the supernatant was evaporated and dissolved in 1 mL 50% (*v*/*v*) of methanol for further *β*-glucosidase (Sigma, product number 49290) hydrolysis and determination.

Lignin extraction was performed from 10 g powdered lyophilized tissues by nitrobenzene oxidation. Lignin is oxidatively cleaved to form aromatic carbonyl compounds, *i.e.*, syringaldehyde and vanillin as the main products. Vanillin and syringaldehyde were used as markers for guaiacyl- and syringyl-type lignin, respectively. The samples were mixed in 27 mL methanol and centrifuged after 10 min. The precipitate was then washed twice with 60 °C deionized H_2O and dried at 50 °C in an oven. The 0.2 g solid residues were mixed in 7 mL basic solution (2 mol/L NaOH and 0.5 mL nitrobenzene), loaded into a stainless-steel reactor and heated up to 170 °C for 2.5 h. In case of high-pressure conditions in this step, we paid close attention to safety. After cooling, the reactor was opened to collect the supernatant, which was then adjusted to pH 3.0 with 1 mol/L HCl and extracted twice with chloroform at room temperature. The combined organic phases were dried with nitrogen and dissolved in 500 μL methanol for further experiments.

2.9. Chemical analysis

Lignan analysis was performed by high-performance liquid chromatography (HPLC) with detection by mass spectrometry (MS) on an Agilent Technologies 1200 system coupled to an Agilent Technologies 6410 quadrupole mass spectrometer (Santa Clara, CA). The enzymatic reaction products of DIRs were subjected to chromatography by a Superchiral R-OZ column (4.6 mm × 250 mm, 5 μm) for chiral analysis using the constructed methods (Supporting Information Table S2). The associated Agilent MassHunter and OpenLAB software packages were used for data collection and analysis. Lignan extracts from LTF1-OVX hairy roots were subjected to chromatography by an Agilent ZORBAX SB-C18 (2.1 mm × 100 mm, 3.5 μm) column (Supporting Information Table S3). Lignin extractions were subjected to chromatography on an Agilent HPLC 1260 equipped with a UV detector and an Agilent tc-C18 column (4.6 mm × 250 mm, 5 μm) (Supporting Information Table S4).

2.10. Stress treatment, qRT-PCR, and heatmap construction

The hairy roots were treated with NaCl (200 mmol/L), H_2O_2 (200 μmol/L), flg22 (1 μmol/L), ABA (50 μmol/L), ethephon (50 μmol/L) and ABA + ethephon (50 μmol/L) separately and then sampled at designated time points for gene expression analysis. Total RNA was extracted using the Plant RNA Extraction kit (Takara, Japan) and then reverse transcribed into complementary deoxyribonucleic acid (cDNA) using the PrimeScript TM kit (Takara, Japan). The PP2A4 gene of *I. indigotica* was selected as the internal reference gene. Primers and standard curves for qPCR analysis are listed (Supporting Information Dataset 1, Fig. S2). The heatmap was constructed with log2 transformed and normalized expression data by TBtools[48].

2.11. Bioinformatics analysis

Phylogenetic analysis was performed using the neighbor-joining method with the pairwise deletion option in MEGA 5.05 (Supporting Information Datasets 2 and 3). The *cis*-elements of promoters (Supporting Information Dataset 4) were predicted using the PlantCARE tool (http://bioinformatics.psb.ugent.be/webtools/plantcare/html).

2.12. Subcellular localization

The gene ORF was fused in a frame with a yellow fluorescent protein (YFP) and driven by the 35S cauliflower mosaic virus promoter. The constructs were introduced into the *A. tumefaciens* strain GV3101 for infiltration and transient expression in *Nicotiana benthamiana epidermal* cells. We collected and recorded the results after 2 days of transformation at an excitation wavelength of 511 nm and an emission wavelength in the range 520−548 nm. The YFP fluorescence signal was imaged using a Leica TCS SP5 laser confocal scanning microscope (Leica Microsystems, Germany).

2.13. β-Glucuronidase staining (GUS) analysis

The gene promoter was collected from the genomic DNA through PCR and subcloned into the *p*CAMBIA1301 vector. The constructs were transformed into the *A. tumefaciens* strain C58C1, which was used for the transformation of hairy roots. Hairy roots were analyzed by histochemical GUS staining. The stained samples were visualized under an Olympus BX43 light microscope (Olympus, Japan).

2.14. Histochemical staining

Histochemical staining was performed on sections cut from the maturation zone of hairy roots. The hairy roots were embedded in 7% agarose before being transversely sectioned at a thickness of 50 μm using a vibratome (Leica VT1000S, Germany). The phloroglucinol-HCl staining method was used to detect the deposition and composition of lignans, lignin, or wall-bound phenolics and derivatives. All sections were observed under an Olympus BX43 microscope (Japan).

2.15. Y1H assay

In Y1H experiments, LTF1 was amplified and cloned into the *p*GADT7-REC2 vector. The sequence containing the GCCGCC elements of the promoter of pathway genes was cloned into the *p*His2.1 vector. The combination of *p*GADT7-REC2-LTF1 and *p*His2.1-GCC was transformed together into the yeast strain Y187 for cultivation on SD-Leu-Trp selection medium. The empty *p*GADT7-REC2 vector and the mutated *p*His2.1-TCC were used as negative controls. Different combinations were transformed into the yeast strain Y187 to verify the binding of LTF1 to the promoters.

2.16. Electrophoretic mobility shift assays

The biotin-labeled oligonucleotides in this experiment were synthesized by the Genewiz company (Suzhou, China). EMSAs were

performed using the EMSA/Gel-Shift Kit (Pierce, USA) according to the manufacturer's instructions. After blotting on a positively charged nylon membrane, a UV cross-linker was used to cross-link the DNA. The biotin-labeled DNA was detected by chemiluminescence and exposed to X-ray film.

2.17. *Luciferase assay*

The coding sequence of LTF1 was subcloned into the *p*GreenII 62-SK vector (Biovector, Beijing, China) to generate the effector, and the promoters of pathway genes were fused into the vector pGreenII 800-LUC (Biovector) to generate reporters. The empty vectors *p*GreenII 62-SK and *p*GreenII 800-LUC were used as controls for the effector and reporter, respectively. The constructs were then separately transformed into *A. tumefaciens* strain GV3101. Then, the incubated cells were harvested by centrifugation and resuspended in an MSS medium with 10 mmol/L methylester sulfonate (MES) and 150 mmol/L acetosyringone. Cultures were then grown to an OD_{600} of 0.6 and incubated at room temperature for 3 h. Effector- and receptor-containing cells were mixed at a ratio of 1:1 and dispensed into tobacco leaves. LUC activity was measured using a cooled CCD imaging system after 2 days (Lumazone 1300B; Roper Scientific, Trenton, NJ, USA). The leaves were sprayed with 1 mmol/L luciferin and placed in darkness for 3 min before luminescence detection. Three independent biological replicates were measured for each sample.

3. Results

3.1. *Stereochemical analysis of lignans in I. indigotica*

Stereochemical differences in the lignans of wild-type *I. indigotica* were investigated (Supporting Information Fig. S3). With the exception of flowers, (±)-lariciresinol is the major constituent of lignans in the vascular-rich organs of *I. indigotica*, including the root, stem, and leaf. Treatment with β-glucosidase significantly increased the lignan content, indicating that lignans were mainly present in the form of glucosides. To characterize the level of lignan synthesis more accurately, the content levels of all lignans in this study were determined based on the aglycone form, which occurs after glycoside hydrolysis. Lignans in roots and flowers have similar stereochemical characteristics, that is, (−)-pinoresinol, (−)-lariciresinol and (+)-secoisolariciresinol are predominant (Supporting Information Fig. S3d), implying the presence of potential (−)-pinoresinol-forming DIR (defined as (−)-DIR) protein which directs the selective synthesis of lignans.

3.2. *Stereoselective synthesis of antiviral lignans in I. indigotica roots*

To completely characterize the whole stereoselective biosynthesis pathway of lignans, the stereochemical function of pathway enzymes DIR, PLR, and UGT was studied.

To predict functional members of the DIR family, an unrooted phylogenetic tree was created based on the amino acid sequences of 19 potential DIRs of *I. indigotica* and 16 known DIRs (Supporting Information Fig. S4, Dataset 2). Cluster I, consisting of four *I. indigotica* DIRs (DIR1, 2, 3, and 4) and four known (−)-DIRs from flax (*Linum usitatissimum*) and *Arabidopsis thaliana,* corresponds to the previously defined DIR-a subfamily[49]. Of these, the high expression of DIR1 and DIR2 in roots suggests their potential involvement in root lignan biosynthesis (Fig. 1a). Recombinant proteins DIR1 and DIR2 were expressed in *pichia pastoris* and then tested for their biochemical function in *in vitro* reaction mixtures containing *Trametes versicolor* laccase for one-electron oxidation and coniferyl alcohol as a substrate. Reactions with both DIR1 and DIR2 had significant stereoselectivity and produced (−)-pinoresinol in enantiomeric excess (ee), which identified DIR1 and DIR2 as (−)-DIR proteins (Fig. 1b). DIR1 and DIR2 produced (−)-pinoresinol in 45.8 ± 2.3% and 71.0 ± 1.8% ee with the addition of 6.4 μmol/L DIR protein, respectively.

To further study the physiological function of DIRs *in vivo*, DIR1-and DIR2-overexpressing hairy roots (DIR1-OVX and DIR2-OVX) of *I. indigotica* were constructed. Quantitative RT-PCR (qRT-PCR) analysis showed that the transcription of DIR1 and DIR2 was successfully increased in the corresponding overexpression hairy roots (Supporting Information Fig. S5). Analysis of stereochemical differences in lignan accumulation indicated that the content of all lignan stereoisomers in DIR-OVX was increased (Fig. 1c−e). Of these, the content of (−)-pinoresinol-derived lignans in DIR1-OVX and DIR2-OVX hairy roots increased to 1.55 ± 0.09 folds (36.5 ± 2.2 μg) and 2.52 ± 0.25 folds (59.2 ± 5.8 μg/g) of control (23.6 ± 1.3 μg/g), respectively (Fig. 1f). Similarly, the content of (+)-pinoresinol-derived lignans (total content of (+)-pinoresinol, (+)-lariciresinol and (−)-secoisolariciresinol), compared to the control (1.0 ± 0.1 μg/g), was increased by 3.05 ± 0.49 folds (3.0 ± 0.5 μg/g) and by 6.91 ± 1.12 folds (6.8 ± 1.1 μg/g) in DIR1-OVX and DIR2-OVX hairy roots, respectively. The increase in content may be a result of the DIR-mediated regioselectivity of the 8−8′ oxidative coupling of coniferyl alcohol[50]. Surprisingly, coniferyl alcohol content was also significantly increased in both DIR1-OVX (7.0 ± 1.1 μg/g) and DIR2-OVX (32.2 ± 13.4 μg/g) hairy roots, which presents an alternative reason for the overall increase in lignan content (Supporting Information Fig. S6a). Unexpectedly, the ee of (−)-pinoresinol-derived lignan in both DIR1-OVX (84.8 ± 2.5%) and DIR2-OVX (79.5 ± 1.5%) hairy roots was slightly decreased compared to the control (92.0 ± 0.9%), which may be due to excess substrate coniferyl alcohol and saturation of DIR function (Supporting Information Fig. S6b)[51]. *In vitro*, a gradual decrease in the ee of (−)-pinoresinol with increasing coniferyl alcohol concentration supports this hypothesis (Fig. S6c). In conclusion, DIR1 and DIR2 as highly expressed (−)-DIR determine (−)-pinoresinol derived lignans as dominant lignan configuration in *I. indigotica* roots (Fig. 1g).

In previous studies, we reported that PLR is the key enzyme that catalyzes the continuous synthesis of lariciresinol and secoisolariciresinol from pinoresinol[28]. Here, we found that PLR also exhibits significant substrate selectivity, which contributes to the preferential accumulation of (−)-lariciresinol and (+)-secoisolariciresinol in roots (Supporting Information Fig. S7). *In vitro* catalytic assays showed that PLR was able to indiscriminately convert (+)-pinoresinol and (−)-pinoresinol to (+)-lariciresinol and (−)-lariciresinol, respectively; however, PLR only showed low activity in stereoselectively catalyzing (−)-lariciresinol to generate (+)-secoisolariciresinol. Thus DIR1/2 and PLR jointly determine that (−)-lariciresinol derived lignans are the dominant form in roots.

Glycosylation is important for the synthesis of many active natural products[52,53]. UDP-glucoside transferase UGT71B2 was previously identified as a key enzyme catalyzing lariciresinol to antiviral lariciresinol glucosides[30,47,54]. However, the activity to

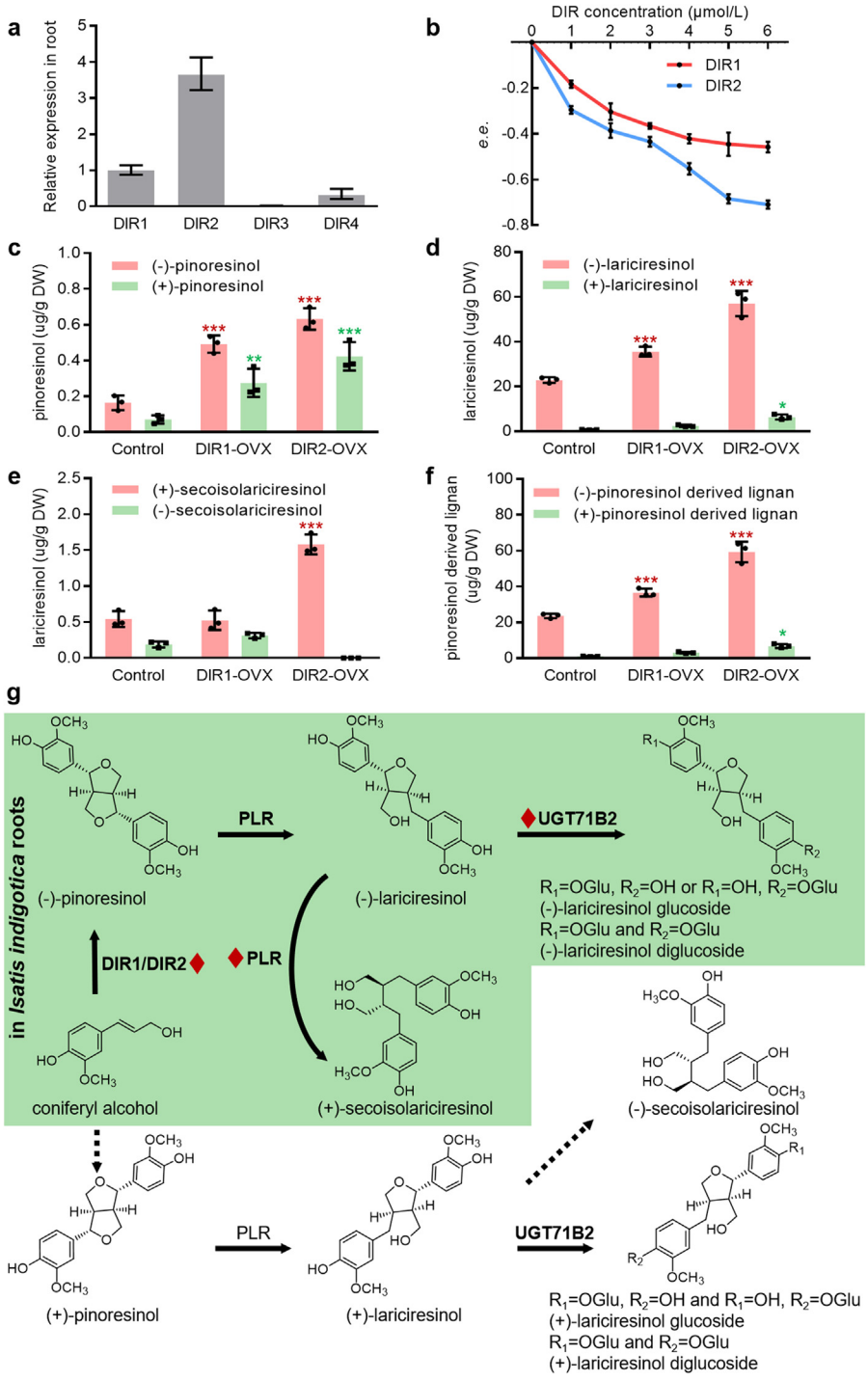

Figure 1 Stereoselective synthesis of lignan glucosides in *I. indigotica* roots. (a) Expression levels of the cluster I DIRs in *I. indigotica*. (b) Enantiomeric excess (ee) of (−)-pinoresinol with increasing amounts of recombinant DIR1 and DIR2. Chiral HPLC−MS/MS analysis of (−)-pinoresinol/(+)-pinoresinol (c), (−)-lariciresinol/(+)-lariciresinol (d), (−)-secoisolariciresinol/(+)-secoisolariciresinol (e) and total pinoresinol-derived lignan (f) contents in transgenic plants. The (−)-pinoresinol-derived lignan content is equivalent to the sum of (−)-pinoresinol, (−)-lariciresinol and (+)-secoisolariciresinol content, and the (+)-pinoresinol-derived lignan content means the sum of (+)-pinoresinol, (+)-lariciresinol and (−)-secoisolariciresinol content. Statistical analysis was performed tween control and over-expressing hairy roots by using Two-way ANOVA multiple comparisons (*$P < 0.05$, **$P < 0.01$, **$P < 0.001$). All data represent the mean of three biologically independent samples and error bars show standard deviation. (g) Stereoselective synthesis of lignan glucosides in *I. indigotica* roots. DIR1 and DIR2 mediates the stereoselective synthesis of (−)-pinoresinol; PLR is able to indiscriminately convert (+)-pinoresinol and (−)-pinoresinol to (+)-lariciresinol and (−)-lariciresinol, respectively, and only show low activity in stereoselectively catalyzing (−)-lariciresinol to generate (+)-secoisolariciresinol; UGT71B2 is able to react with both configurations of lariciresinol and also displayed stereoselectivity, favoring reaction with (+)-lariciresinol over (−)-lariciresinol. In conclusion, (−)-pinoresinol-derived ligans, including (−)-lariciresinol, (+)-secoisolariciresinol and (−)-lariciresinol

different stereo configurations of lariciresinol remains to be investigated. To validate the stereoselectivity of UGT71B2, recombinant UGT71B2 expressed in *E. coli* was reacted with totally racemic (±)-lariciresinol as the sugar-acceptor, producing two glucosides (peaks 8 and 9) and one diglucoside (peak 10) (Supporting Information Fig. S8a). Owing to the difficulty in the chiral separation of glucosides by chromatographic analysis, the remaining concentrations of substrates were used to analyze the stereoselectivity of UGT71B2 (Fig. S8b). The unequal amounts of remaining substrates (+)-lariciresinol and (−)-lariciresinol indicated that UGT71B2 was able to react with both configurations and also displayed stereoselectivity, favoring reaction with (+)-lariciresinol over (−)-lariciresinol (Fig. S7).

In conclusion, the stereo configuration of lignans in *I. indigotica* is determined by the first key enzyme DIR from the beginning, and PLR and UGT71B2 further refine it, ultimately achieving lignan accumulation with specific stereoconformation, which determines that the dominant antiviral lignan in *I. indigotica* roots is (−)-lariciresinol derived lignans including (−)-lariciresinol glucosides (Fig. 1g).

3.3. DIRs enhance stress resistance by mediating an increase in lignan and lignin content

As the first key enzyme of the lignan pathway, 22 *At*DIRs in *A. thaliana* were shown to exhibit specific expression patterns in different tissues and in response to different hormones[55]. In parallel, the expression of different *At*DIRs significantly varies following biotic and abiotic stress-related treatments[50,55]. Each DIR in spruce, conifer, and sugarcane also shows its own unique expression patterns in different tissues and in response to different stress and hormone treatments[49,56,57]. These results imply that DIR may be the key gene for plant lignans to respond to environmental stresses, but the transcriptional regulation mechanism has not been well explained.

To investigate whether the DIRs contribute to plant defense through lignan biosynthesis, we first tested their response to biotic and abiotic stresses. NaCl (300 mmol/L) and H_2O_2 (200 μmol/L) treatments were used to assess salt and oxidative tolerance, respectively; Flg22 (1 μmol/L) treatment was used to simulate biotic stress for triggering immunity (Fig. 2). Upon stress stimulation, there was a rapid and robust increase in the expression of DIRs, especially DIR1 (Fig. 2a). Compared with DIR2, the expression of DIR1 was more significantly increased by 55.12 ± 25.45 folds at 6 h following H_2O_2 treatment. NaCl and Flg22 increased the expression of DIR1 by 5.79 ± 3.08 and 31.32 ± 7.04 folds at 0.5 h, respectively. The expression of DIR2 was induced at 0.5, 6, and 0.5 h after the different stress treatments. These results suggest that DIR1 expression may play an important role in plant defense, especially in response to oxidative stress.

We next investigated the stress resistance of control and overexpression hairy roots (Fig. 2b). After 9-day cultivation, the growth rate and biomass of DIR1-OVX and DIR2-OVX hairy roots were significantly higher than those in the control following NaCl and H_2O_2 treatment, suggesting that DIR1 and DIR2 were involved in tolerance to abiotic stresses. Flg22 is often used to induce plant immune responses caused by microorganisms without causing actual damage to the plants. Although the hairy roots of the control and overexpression lines had similar growth rates (biomass of ∼10 g), the inducible expression by Flg22 implied the involvement of the DIR proteins in response to biotic stresses (Fig. 2a). In addition to the increase of lignan levels in DIR overexpressing roots (Fig. 1c−e), we also found an increase in lignin content (both S- and G-type lignin) (Supporting Information Fig. S9), which is important for plant defense[58]; furthermore, S/G ratio values decreased from 1.64 to 1.17 and 1.45 in the DIR1-OVX and DIR2-OVX hairy roots, respectively (Fig. 2c and d), which could be caused by the increased content of coniferyl alcohol (Supporting Information Fig. S6). Furthermore, fluorescence localization of GFP indicated that both DIR1 and DIR2 specifically localize in the cell periphery, which allows them to perform biological functions extracellularly (Fig. 2e). These results suggest that DIRs, especially DIR1, participate in the regulation of stress resistance by mediating lignan and lignin biosynthesis in *I. indigotica* (Fig. 2c).

3.4. LTF1 positively regulates stress resistance through lignan biosynthesis

Given that a typical ERF binding element (GCCGCC box) was found in the promoter of DIR1, the ERF transcription factor may regulate DIR1 expression and lignan synthesis (Supporting Information Fig. S10). ERF transcription factors play an important role in the response to biotic and abiotic stresses[59−61]. Through "gene-metabolite" network analysis, we previously predicted that an ERF transcription factor, lignan biosynthesis-associated transcription factor 1 (LTF1), which is highly expressed in roots, was correlated with lignan biosynthesis[17]. Comparison of the amino acid sequences along with phylogenetic analysis indicated that LTF1 was homolog to the unknown ERF1B of other Cruciferae (*Rs*ERF1 of *Raphanus sativus* and *Br*ERF1 of *Brassica rapa*) and seemingly clustered with *At*ERF1, which was thought in plant defense with unknown mechanisms[62] (Fig. 3a, Supporting Information Dataset 3). LTF1 subcellular localization was determined by transiently expressing an N-terminal fusion of ERF1 to GFP in *N. benthamiana* leaves by agroinfiltration. The specific fluorescence localization of the LTF1-GFP fusion protein indicated that it functioned as a transcription factor in the nucleus (Fig. 3b). The transcriptional pattern showed that LTF1 was highly expressed in roots, which was similar to the accumulation characteristics of lignans (Fig. 3c and d).

Biosynthesis of antiviral lignans in *I. indigotica* is originated from phenylalanine and is accomplished by three cooperative pathways including the phenylpropanoid pathway, aromatic alcohol pathway, and lignan pathway (Fig. 3e). The gene transcript abundance detected by qPCR showed that the expression pattern of LTF1 was very similar to that of DIR1, as well as some other pathway genes (*e.g.,* PLR and CCR) (Fig. 3f). These results suggest that LTF1 is strongly associated with lignan biosynthesis in roots and is a strong candidate gene for mediating stress resistance. By the way, the low expression levels of DIR1 and

glucosides, are the primary lignan component in *I. indigotica* roots. Green background represents stereoselective pathway of antiviral lignans in *I. indigotica* roots. Arrows represent the reactions *in vitro*. Dotted arrows represent reactions that do not happen in *I. indigotica* roots. The red squares represent the stereoselective steps in the root.

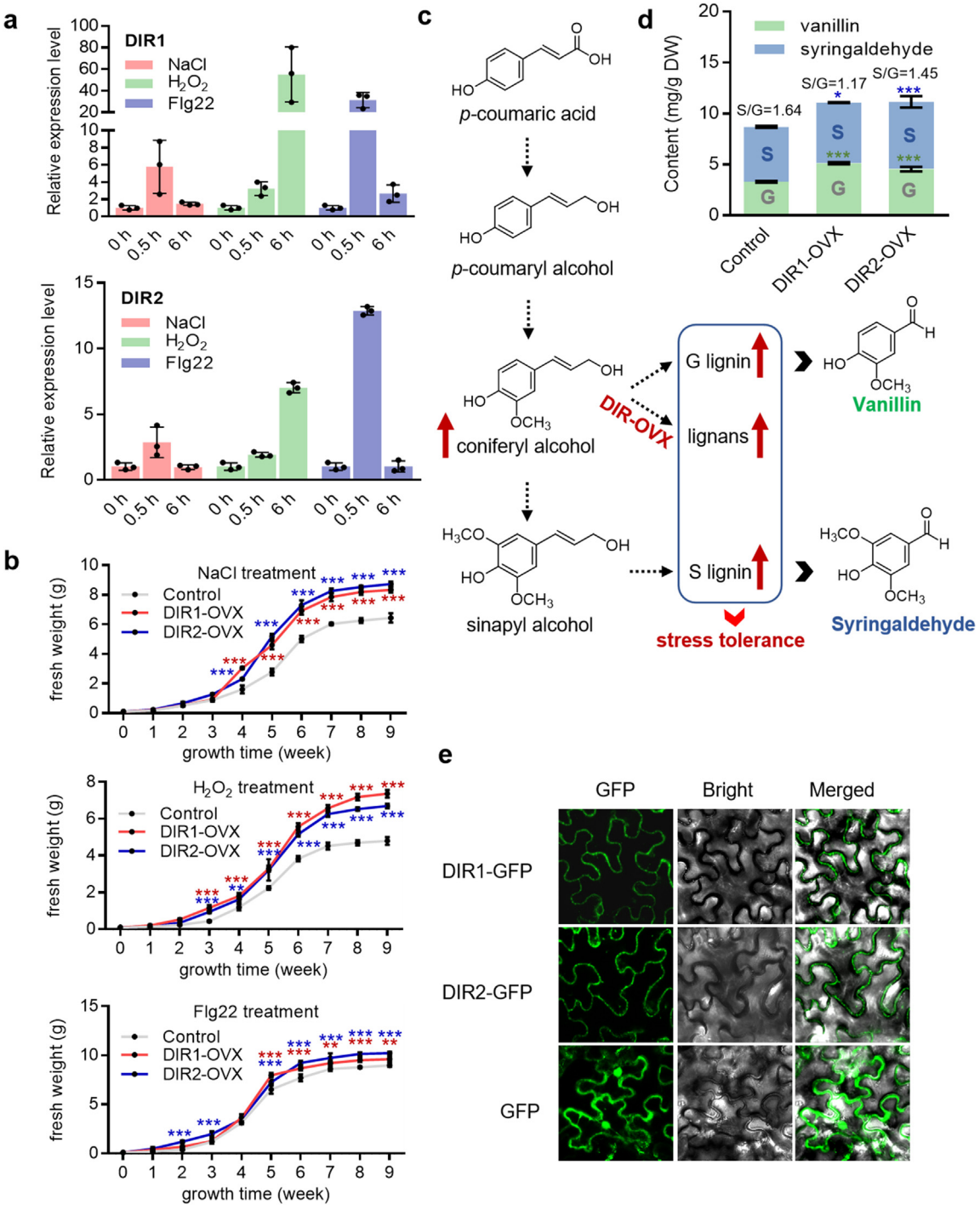

Figure 2 Stress resistance by DIR1 and DIR2 in plants. (a) qRT-PCR analysis of DIR1 and DIR2 induction by NaCl, H_2O_2 and Flg22 treatment. (b) Growth curves of control and overexpression hairy roots after NaCl, H_2O_2 and Flg22 treatment. (c) Metabolic mechanism by which DIR exerts stress resistance. (d) Lignin analysis in control and overexpression hairy roots. (e) Subcellular localization of DIR1 and DIR2 in *N. benthamiana* leaf epidermal cells. Statistical analysis was carried out by using Two-way ANOVA (**$P < 0.005$, ***$P < 0.001$).

DIR2 are consistent with the weak stereoselective synthesis of (−)-pinoresinol derived lignans in stems and leaves (Supporting Information Fig. S3e and f).

From the above screening, LTF1 was selected and further characterized. The expression of LTF1 was rapidly induced by salt, H_2O_2, and Flg22 over 6 h, and the expression peaked at 0.5, 6, and 0.5 h, respectively, for the different stress treatments (Supporting Information Fig. S11). The expression of defense- and stress-responsive genes in response to biotic and abiotic stresses are modulated by the antagonistic interactions between multiple components of the ABA and ethylene signaling pathways[63,64]. Considering that phytohormones play an important role in the

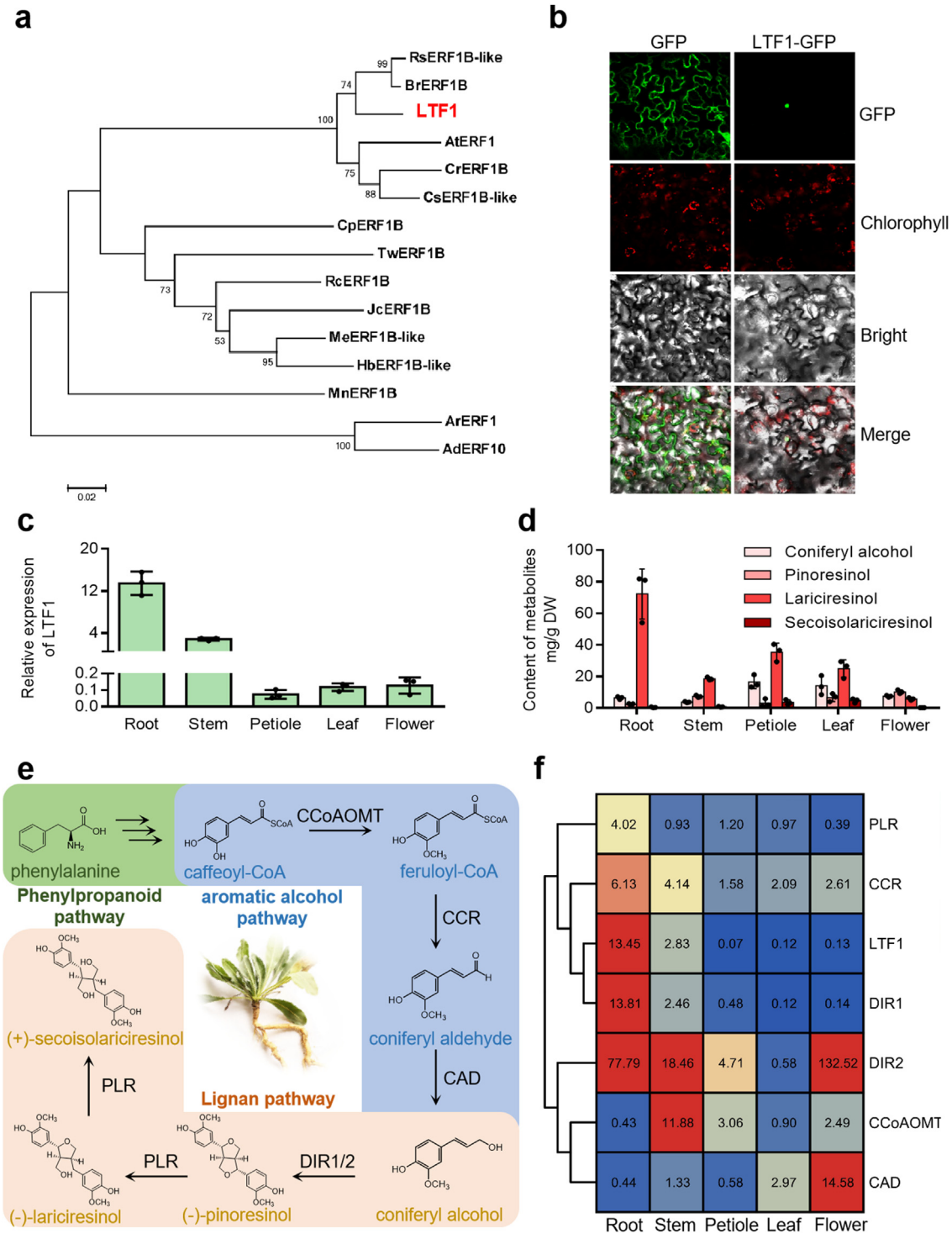

Figure 3 Expression patterns of LTF1. (a) Phylogenetic analysis of LTF1. (b) Transient expression of LTF1-GFP fusion in *N. benthamiana* leaves. Image shows nuclear localization of LTF1-GFP. LTF1 expression (c) and lignan contents (d) in different organs of *I. indigotica*. (e) Biosynthetic pathway of lignans. (f) Cluster analysis of gene expression patterns in different organs. Gene expression levels from low to high are represented by the transition from blue to red. Values represent relative expression levels.

response to stresses, we asked whether ethephon (ET) and ABA affect the induction of LTF1 expression. The results of qRT-PCR indicated that ET significantly triggered LTF1 expression after 1 h of treatment, which was highly similar to the expression pattern of DIR1 and DIR2 (Fig. 4a). The response intensity of DIR1 and DIR2 to ET was significantly higher than that of other pathway genes, implying that DIR may be a key step of the lignan pathway in response to environmental changes. Conversely, LTF1 was inhibited after 0.5 h of ABA treatment and gradually recovered at later time points (Fig. 4b). It should be noted that DIR1 and DIR2

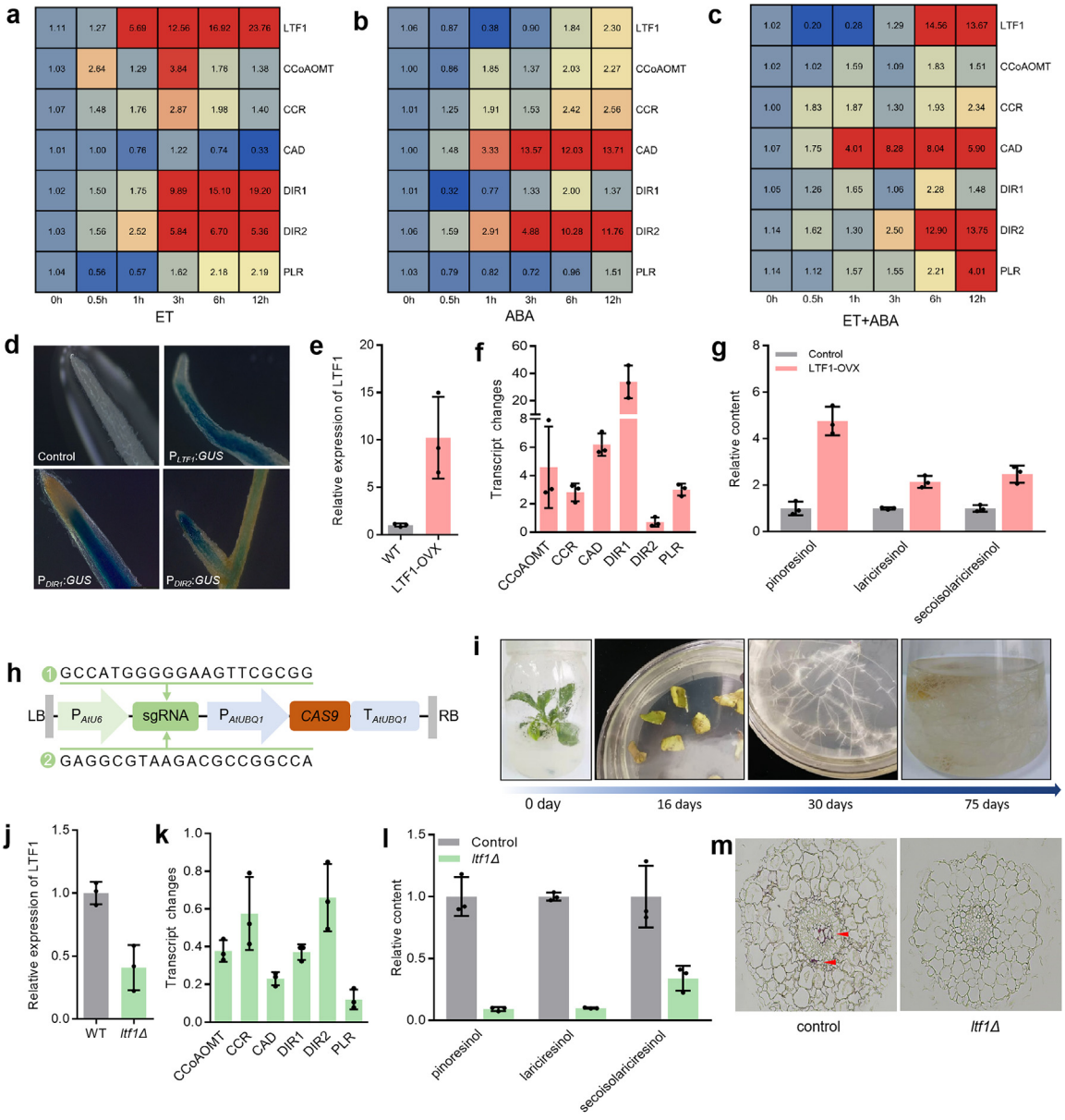

Figure 4 LTF1 positively regulates lignan biosynthesis in the roots of *I. indigotica*. Heatmap of the expression patterns of lignan pathway genes in response to ET (a), ABA (b) and ET + ABA (c). (d) Analysis of GUS activity driven by the LTF1, DIR1 and DIR2 promoters in hairy roots. (e) Relative expression of LTF1 in LTF1-OVX hairy roots. (f) The changes in transcript expression of ligan pathway genes in LTF1-OVX hairy roots. (g) The relative level of lignans in LTF1-OVX hairy roots compared to the control. (h) The design of sgRNA for LTF1 editing. (i) The induction and cultivation *I. indigotica* hairy roots. (j) Relative expression of LTF1 in *ltf1Δ* hairy roots. (k) The changes in transcript expression of ligan pathway genes in *ltf1Δ* hairy roots. (l) The relative level of lignans in *ltf1Δ* hairy roots compared to the control. (m) Cross sections of hairy roots stained with phloroglucinol-HCl.

had completely different responses to ABA, and only DIR1 maintained the same expression pattern as LTF1. Furthermore, LTF1 induction by ET treatment was suppressed by ABA, which was again consistent with DIR1 (Fig. 4c). These results imply that LTF1 may regulate lignan biosynthesis through DIR1, rather than DIR2, and mediate stress resistance. The GUS staining assays also showed that P_{LTF1}:GUS and P_{DIR1}:GUS expression principally occurred in the vascular strand of mature root tissues, while P_{DIR2}:GUS was principally expressed in root tips, which further suggests a potential regulatory relationship between LTF1 and DIR1 (Fig. 4d).

To test this conjecture, we first overexpressed LTF1 in LTF1-OVX hairy roots, where the expression level of LTF1 was successfully increased 10.23 ± 4.31 folds compared to the control (Fig. 4e). As expected, DIR1 expression levels were dramatically increased by 33.80 ± 12.00 folds (Fig. 4f). Conversely, the expression level of DIR2 in the LTF1-OVX hairy root was only 0.72 ± 0.33 folds of that in the control. Clearly, these results indicated a significant positive regulation of DIR1 by LTF1. Metabolite analysis indicated a 4.76 ± 0.61 folds increase in pinoresinol content in the LTF1-OVX hairy root compared to the control (Fig. 4g). The increase of pinoresinol content was also transmitted to downstream, which increased the accumulation levels of lariciresinol and secoisolariciresinol by 2.15 ± 0.26 and 2.47 ± 0.37 folds, respectively. The results of

qRT-PCR indicated that abiotic and biotic stresses also triggered the LTF1 expression, which was very similar to the response of DIR1 (Fig. S11). Growth curve analysis showed that overexpression of LTF1 made hairy roots grow better under the stress treatments (Supporting Information Fig. S12). Based on these results, we conclude that LTF1 can respond to environmental stresses through phytohormones, thereby positively regulating DIR1 expression and lignan biosynthesis to increase stress resistance.

To verify the necessity of LTF1 in stress resistance by lignans, we tried to mutate the LTF1 gene in hairy roots through the CRISPR/Cas9 system. Based on the previously constructed genome of *I. indigotica*, two potential high-scoring 20-bp sequences followed by the NGG (PAM sequence) from the open reading frame (ORF) of LTF1 were designed and cloned into a construct harboring a chimeric single guide RNA (sgRNA) driven by the *A. thaliana* U6-26 promoter (P_{AtU6}) (Fig. 4h). The constructs were transformed into *A. rhizogenes* to infect wounded young leaves for generating hairy roots (Fig. 4i). Heterozygous and biallelic mutations that produced superimposed sequence chromatograms of LTF1 were decoded using the Degenerate Sequence Decoding method[65]. Sequencing data revealed that sgRNA1 and sgRNA2 generated 10 and 12 hairy root lines containing mutations with corresponding mutation rates of 52% and 47%, respectively (Supporting Information Table S1). Of these, seven mutations were homozygous, with mutations occurring in the same DNA locus in both alleles (Supporting Information Fig. S13). Others were non-homozygous mutations, including six heterozygous mutations (wild type/single mutation) and nine biallelic mutations (two distinct variations). Most mutations generated by sgRNA1 caused a single nucleotide insertion of A or T, whereas many mutations produced by sgRNA2 had multiple nucleotide deletions. Three hairy root lines (lines 1−5, 1−18, and 2-1) with significantly reduced expression of LTF1 were selected by qRT-PCR and used for further analysis (Fig. 4j). The qPCR results showed that the expression of lignan pathway genes was reduced to varying extents upon mutation of LTF1 (Fig. 4k). The expression of DIR1 and DIR2 in *ltf1Δ* hairy roots was 0.37 ± 0.04 folds and 0.66 ± 0.18 folds of that in control hairy roots. Combined with the results of tissue localization experiments, these results show that DIR1 expression is likely controlled by LTF1, while LTF1 does not regulate the expression of DIR2 (Fig. 4d). Unexpectedly, the expression of other pathway genes was also inhibited in *ltf1Δ* hairy roots, especially PLR, which was decreased most significantly to only 0.12 ± 0.05 folds of the control, suggesting that LTF1 is essential for the normal expression of PLR. Metabolite analysis revealed that the contents of pinoresinol, lariciresinol, and secoisolariciresinol were significantly reduced to 0.09 ± 0.02, 0.10 ± 0.01 and 0.34 ± 0.10 folds of the control, respectively (Fig. 4l). Phloroglucinol-HCl staining of cross sections of hairy roots shows that the *ltf1Δ* hairy root had a weaker browning of vascular regions visually compared to the control, which reveals that LTF1 is necessary for the accumulation of lignans, lignin, and/or wall-bound phenolics and derivatives (Fig. 4k). Thus, it is reasonable that the growth of *ltf1Δ* hairy roots was worse than that of the control (Supporting Information Fig. S12). Based on these results, we preliminarily conclude that LTF1 plays a stress-resistant function by regulating the expression of the lignan pathway gene DIR1, and LTF1 is also critical for the expression of other genes in the pathway, especially PLR.

3.5. *LTF1 directly upregulates DIR1 for stress defense*

Previous results indicated that the expression of the stress resistance-related DIR1, instead of DIR2, was significantly elevated in the LTF1-OVX line and decreased in the *ltf1Δ* line. To investigate the underlying mechanisms by which LTF1 regulates DIR1 expression and lignan biosynthesis, we found a typical ERF binding element (GCCGCC box) in the DIR1 promoter (Supporting Information Fig. S9). Considering that the homolog of LTF1 in other plants, can directly regulate gene expression by binding to the GCC box, we speculate that DIR1 may also be directly regulated by LTF1[66−69]. To test this hypothesis, the yeast one-hybrid assay (Y1H), electrophoretic mobility shift assay (EMSA), and transient luciferase analysis were performed.

We first performed Y1H assays to determine whether LTF1 was able to directly bind the DIR1 promoter sequence (P_{DIR1}) containing the GCC box. Y1H assays were carried out with the addition of 50 mmol/L 3-AT to inhibit the self-activating effect (false positive result) and the results showed that LTF1 was indeed able to bind the 3 × GCC element in the DIR1 promoter to activate the expression of the reporter gene HIS3, which allowed yeast to grow on selection plates (-T/-L/-H/+50 mmol/L 3-AT) (Supporting Information Fig. S14, Fig. 5a). Conversely, all negative controls, including the use of the mutated 3 × TCC element ($P_{mutDIR1}$), failed to grow clones on the selection plate.

Next, P_{DIR1} was used as a labeled probe for EMSAs, and the results showed a distinct shift band of the DNA-LTF1 complex (column 2) (Fig. 5b). Binding activity was gradually diluted by the unlabeled probes (columns 3−6) and the labeled mutated probes with the TCCTCC box (columns 7−10). These results provide strong evidence that LTF1 binds to the native promoter of DIR1 through the GCCGCC *cis*-element.

To further verify whether LTF1 positively regulates the transcription of DIR1, we performed transient expression assays in *N. benthamiana* leaves (Fig. 5c). The DIR1 promoter region P_{DIR1} was used to drive the luciferase gene (*LUC*) as the reporter, and LTF1 was overexpressed under the control of the CaMV35S promoter ($P_{CaMV35S}$) as the effector. Detection of LUC luminescence indicated that overexpression of LTF1 ($P_{CaMV35S}$:LTF1) significantly increased the LUC signal of the reporter (P_{DIR1}:LUC) compared to controls lacking $P_{CaMV35S}$:LTF1.

In conclusion, combined with the analysis of hairy roots, these results showed that LTF1 can transcriptionally upregulate lignan biosynthesis through the first key enzyme DIR1.

4. Conclusions and discussions

In addition to the involvement in the process of plant defense, lignans have various activities to protect human health. Lignans are the main antiviral components in the *I. indigotica* root[25,26]. However, the stereo configuration of lignans and their stereoselective biosynthetic pathway in *I. indigotica* are unclear, which may threaten the safety of medicine use and make it difficult for plant improvement. Although lignans have been considered key players in plant stress resistance[9], the long-sought-after mechanism of lignan biosynthesis in response to the environment has remained elusive.

In this study, we systematically identified the stereoselective biosynthesis of lignans in the *I. indigotica* root, which determined (−)-lariciresinol glucosides as antiviral lignans. First, we found that two of the 19 DIRs (DIR1 and DIR2) were highly expressed

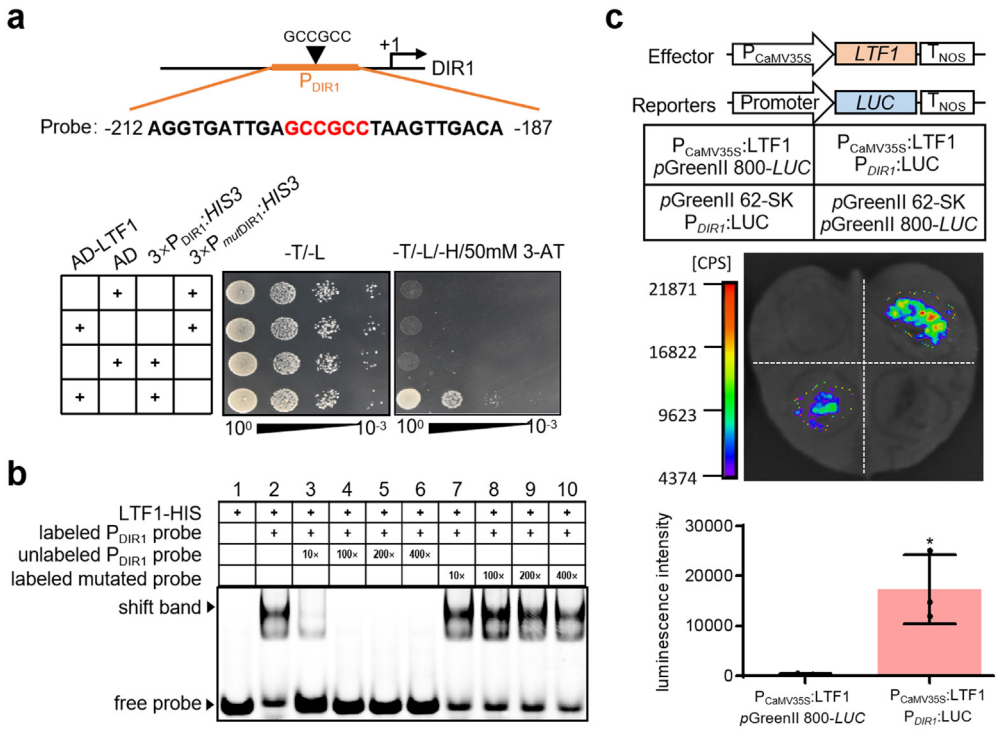

Figure 5 LTF1 directly binds to the GCC box of the DIR1 promoter and activates its transcription. (a) Promoter of DIR1. (b) Y1H assays showing that the LTF1 protein binds to triple (3 ×) tandem repeats in the P_{DIR1} sequence of the DIR1 promoter. Black triangles represent the dilution ratio of the yeast suspension. (c) EMSAs showing that LTF1 specifically binds to the P_{DIR1} sequence of the DIR1 promoter. An excess of the unlabeled probe (lines 3−6) and labeled mutated probe (lines 7−10) were used as competitors. The free and bound DNA bands are indicated by black arrows. (d) Transient luciferase analysis showing that higher luminescence intensity was observed following coexpression of *LTF1* and P_{DIR1}:*LUC*. Quantitative analysis of luminescence intensity was performed. Statistical analysis was carried out by using Student's *t*-test (one-tailed, $*P < 0.05$).

in the *I. indigotica* root, showed stereoselectivity *in vitro* by guiding the synthesis of (−)-pinoresinol, and showed significant regioselectivity *in vivo*, thereby promoting the accumulation of lignans in roots (Fig. 1). In the consequent step, PLR showed stereoselectivity for the substrate and catalyzed the formation of specific configurations of (−)-lariciresinol and (+)-secoisolariciresinol. The last step of antiviral (−)-lariciresinol glucoside biosynthesis involved the reaction of UGT71B2 with (−)-lariciresinol. The biochemical functions of DIR1, DIR2, PLR, and UGT71B2 explain the lignan composition in the roots of *I. indigotica* (Supporting Information Fig. S3).

In addition, we showed that overexpression of DIR1 and DIR2 increased biosynthesis of lignan and lignin, resulting in significantly enhanced stress tolerance of hairy roots to NaCl, H_2O_2, and Flg22 (Fig. 2). Additionally, we observed a high consistency between the expression patterns of DIR1 and LTF1 (tissue localization, phytohormone response, and stress induction). We found that LTF1 directly activates DIR1 to enhance plant defense ability through lignan biosynthesis, which sheds light on the potential application of lignan biosynthesis in improving plant stress tolerance (Figs. 4 and 5). As shown in Fig. 4, the expression levels of some other pathway genes were changed in LTF1 overexpressed and mutated plants. Among the gene promoters available to us (CCoAOMT, DIR2 and, PLR) (Supporting Information Dataset 4), only the DIR2 promoter contains many *cis*-elements related to stress response and binding sites of MYB transcription factors (Supporting Information Fig. S10), which imply the different regulatory mechanisms for DIR2 expression. The fact that DIR2 shows a completely different response to phytohormones than DIR1 (Fig. 4a−c), and CCoAOMT and PLR are also less responsive to phytohormones, support this hypothesis. Notably, although DIR2 has a similar biochemical function to DIR1, the response level to stresses of DIR2 is much weaker than that of DIR1 (Fig. 2a), indicating that DIR1 is more like a supplement for DIR2 under environmental stresses, making lignan synthesis more efficient. Given that methyl jasmonate (MeJA) is a vital plant cellular regulator that mediates defense responses against biotic and abiotic stresses, including drought, salinity, and pathogen infection[70,71], the MeJA induced transcript abundance of all identified genes of the lignan pathway and DIR family members were analyzed through the previously constructed transcriptome data (Supporting Information Fig. S15)[39]. As expected, all genes of the lignan pathway are highly expressed in the root. The transcript abundance of five members of the DIR family (DIR1, DIR2, DIR9, DIR11, and DIR17) is higher in the root. Interestingly, of the all identified lignan pathway genes, only DIR1 can significantly respond to MeJA treatment. Conversely, the expression of DIR2 is always at a relatively high level in the root. These results confirm our conclusion that DIR1 is vital for the environmental response of *I. indigotica* roots through regulating lignan biosynthesis.

We developed a CRISPR/Cas9-guided gene-editing system for *I. indigotica* to construct *ltf1Δ* hairy roots, which showed extreme lignan defects and stress susceptibility (Fig. 4). Conversely, the content of lignan and the defense against stresses were significantly increased in LTF1-OVX hairy roots. Based on this data, we

propose a working model of the *I. indigotica* stress response in which LTF1 responds to environmental stresses through phytohormone-related signal transduction, directly binding to the DIR1 promoter and activating DIR1 expression in the cell periphery of vascular regions in mature roots and further triggering the accumulation of lignin and the stereoselective synthesis of lignans (Fig. 6). Furthermore, the increased content of lignan and lignin lead to higher stress resistance in *I. indigotica*.

Although transcription factors AP2/ERF049 of Soloist subfamily and WRKY34 in our previous studies have been proven to affect lignan synthesis through PAL and 4CL of phenylpropanoid pathway, and CCR of aromatic alcohol pathway, which all are not direct regulation of the lignan pathway[40,41]. The LTF1 of the ERF subfamily in this study is the first transcription factor directly activating lignan biosynthesis through DIR, the common key gene of all lignan biosynthesis in plants. As reported, DIR and homologs thereof are found in at least 104 studied terrestrial plants but not in aquatic organisms (such as algae), bacteria and mammals, indicating that the DIR family may originate from and be present in vascular plants to withstand the stresses on land[72]. Most members of the DIR family in *A. thaliana* (15 of 22) and *I. indigotica* (9 of 19) are highly expressed in roots[16,55], further implying that vascular plants may have evolved the DIR family and their specific functions during the process of land colonization. As an increasing number of DIR proteins have been characterized, there is no doubt that some DIRs with regio- and stereoselectivity mediate the specific production of (+)- or (−)-pinoresinol[32,50,73–75]. In addition to the identified pinoresinol-forming DIRs, there are at least 20, 35, and 17 DIRs with unknown functions in *A. thaliana*, *Picea spruce*, and *I. indigotica*, respectively. Considering that their expression levels all show temporal and spatial specificity, as well as inducibility, it is reasonable to speculate that they could have specific biological functions in response to stress. For example, a Dirigent domain-containing protein identified in *A. thaliana* mediates resistance to floods and droughts by regulating the formation of the Casparian strip in the root[34]. Therefore, more efforts are needed to unravel the mystery of DIR functions in plant defense. This study verified that the root-specific DIRs (DIR1 and DIR2) of *I. indigotica* are involved in stress resistance (salt, oxidative and pathogen stress in this study) *in vivo* through overexpression experiments, and this finding suggests that the DIRs in other plants with the same biochemical function in mediating the selective biosynthesis of lignans should play a role in stress resistance. The inducibility of these genes by phytohormones and stresses further supports this hypothesis[49,55–57]. In the signal transduction process, whether in response to biotic stress or abiotic stress, H_2O_2 is an important signaling molecule, and H_2O_2 is detrimental to biomolecules when its levels exceed the cellular capacity for detoxification[76]. As polyphenolic compounds, lignans may achieve stress resistance by eliminating ROS, and this idea has been verified by pharmacological experiments[77,78]. On the other hand, the free radical oxidative coupling reaction of coniferyl alcohol to generate pinoresinol can consume H_2O_2, and the increase in DIR expression can significantly enhance the number of reactions (Fig. 1 and Supporting Information Fig. S5). Thus, the expression of DIRs is significantly upregulated under stresses in *I. indigotica*, and this probably enhances the consumption of H_2O_2 by the free radical oxidation coupling reaction, which in turn increases resistance to stresses.

In addition to stress defense for plants, lignans with the specific stereo configuration often have important physiological functions in humans, such as the functions of (−)-podophyllotoxin as pharmaceuticals for cancer treatment[79,80]. In particular, chemically-modified derivatives of (−)-podophyllotoxin, teniposide, etoposide, and etoposide are widely used in cancer chemotherapy[81–83]. Although lignan glucosides are the main antiviral active component of *I. indigotica*, their stereo configurations are

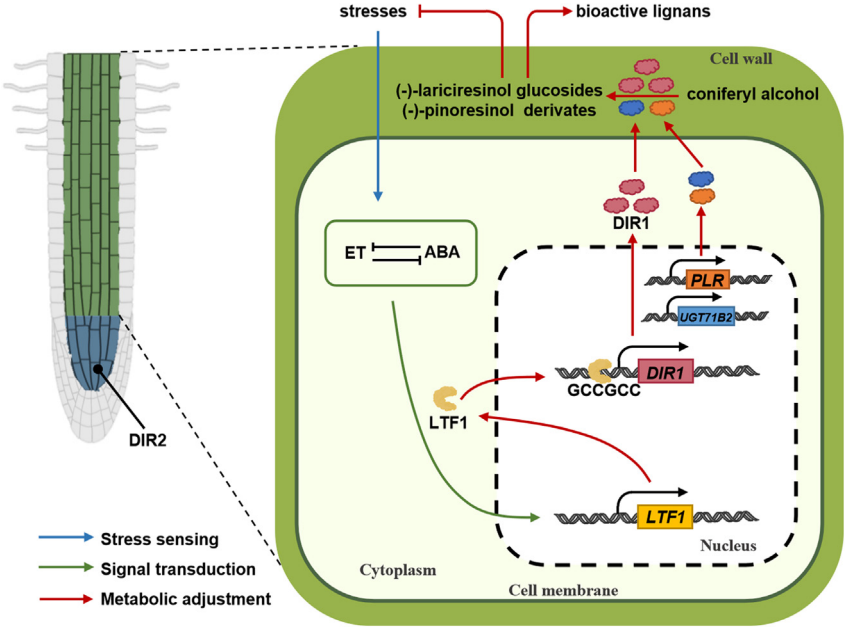

Figure 6 Proposed working model depicting the roles of LTF1-DIR1 module in lignan biosynthesis and stress defense. The stresses are sensed by diverse receptors and the perceived signals further trigger stress-specific signal transduction. The multilevel transduction ultimately activates LTF1, which further binds to the promoter of DIR1 to up-regulate the expression of DIR1. The DIR1 protein is specifically localized in the cell periphery of vascular regions in mature roots to direct the accumulation of lignin and the stereoselective synthesis of lignans and thus plays a role in stress defense.

still unclear. This study indicated that 3 enzymes (DIR, PLR, and UGT) with stereoselectivity cooperate to synthesize (−)-pinoresinol derived lignans and antiviral (−)-lariciresinol glucosides in *I. indigotica* roots. The overexpression of DIR1 and DIR2 in hairy roots proved that DIR1 and DIR2 were involved in the *in vivo* synthesis of (−)-pinoresinol derived lignans, and also significantly increased the content of antiviral lignans and stress resistance. Therefore, we believe that DIR is an ideal target to engineer plants that accumulate valuable lignans, which will increase the content of lignans while also improving stress resistance.

Acknowledgments

The authors would like to acknowledge Professor Jiankang Zhu and his lab at the Shanghai Center for Plant Stress Biology, Chinese Center for Plant Stress Biology, for providing the CRISPR/Cas9 system plasmids. All authors declare no competing financial or nonfinancial interests. This work was funded by the National Natural Science Foundation of China (grant Nos. 82225047, 32000231, 31970316, and 32170274), the National Key Research and Development Program of China (grant no. 2022YFC3501703), Shanghai Science and Technology Development Funds (23QA1411400, China) and Key project at central government level (The ability establishment of sustainable use for valuable Chinese medicine resources, 2060302).

Author contributions

Lei Zhang, Wansheng Chen, and Ruibing Chen conceived the original research. Ruibing Chen, Jian Yu, and Liang Xiao designed and performed experiments. Qing Li and Luyao Yu analyzed the data. Ying Xiao, Junfeng Chen., Shouhong Gao, and Xianghui Chen performed the metabolic analysis. Ruibing Chen and Henan Zhang wrote the manuscript. All authors contributed to the preparation of the manuscript.

Conflicts of interest

The authors declare that the research was conducted in the absence of any commercial or financial relationships that could be construed as a potential conflict of interest.

Appendix A. Supporting information

Supporting data to this article can be found online at https://doi.org/10.1016/j.apsb.2023.08.011.

References

1. Bailey-Serres J, Parker JE, Ainsworth EA, Oldroyd GED, Schroeder JI. Genetic strategies for improving crop yields. *Nature* 2019;**575**:109−18.
2. Zhang H, Zhu J, Gong Z, Zhu JK. Abiotic stress responses in plants. *Nat Rev Genet* 2022;**23**:104−19.
3. Noctor G, Lelarge-Trouverie C, Mhamdi A. The metabolomics of oxidative stress. *Phytochemistry* 2015;**112**:33−53.
4. Ren J, Wu Y, Zhu Z, Chen R, Zhang L. Biosynthesis and regulation of diterpenoids in medicinal plants. *Chin J Nat Med* 2022;**20**:761−72.
5. Chen R, Bu Y, Ren J, Pelot KA, Hu X, Diao Y, et al. Discovery and modulation of diterpenoid metabolism improves glandular trichome formation, artemisinin production and stress resilience in *Artemisia annua*. *New Phytol* 2021;**230**:2387−403.
6. Tohge T, Fernie AR. Leveraging Natural variance towards enhanced understanding of phytochemical sunscreens. *Trends Plant Sci* 2017;**22**:308−15.
7. Cesarino I. Structural features and regulation of lignin deposited upon biotic and abiotic stresses. *Curr Opin Biotechnol* 2019;**56**:209−14.
8. Teponno RB, Kusari S, Spiteller M. Recent advances in research on lignans and neolignans. *Nat Prod Rep* 2016;**33**:1044−92.
9. Villari C, Herms DA, Whitehill JG, Cipollini D, Bonello P. Progress and gaps in understanding mechanisms of ash tree resistance to emerald ash borer, a model for wood-boring insects that kill angiosperms. *New Phytol* 2016;**209**:63−79.
10. Haller HL, McGovran ER, Goodhue LD, Sullivan WN. The synergistic action of sesamin with pyrethrum insecticides. *J Org Chem* 1942;**7**:183−4.
11. Harmatha J, Dinan L. Biological activities of lignans and stilbenoids associated with plant-insect chemical interactions. *Phytochemistry Rev* 2003;**2**:321−30.
12. Youn B, Moinuddin SG, Davin LB, Lewis NG, Kang C. Crystal structures of apo-form and binary/ternary complexes of *Podophyllum secoisolariciresinol* dehydrogenase, an enzyme involved in formation of health-protecting and plant defense lignans. *J Biol Chem* 2005;**280**:12917−26.
13. Patten AM, Davin LB, Lewis NG. Relationship of dirigent protein and 18s RNA transcript localization to heartwood formation in western red cedar. *Phytochemistry* 2008;**69**:3032−7.
14. Carpinella MC, Ferrayoli CG, Palacios SM. Antifungal synergistic effect of scopoletin, a hydroxycoumarin isolated from *Melia azedarach* L. fruits. *J Agric Food Chem* 2005;**53**:2922−7.
15. Schroeder FC, del Campo ML, Grant JB, Weibel DB, Smedley SR, Bolton KL, et al. Pinoresinol: a lignol of plant origin serving for defense in a caterpillar. *Proc Natl Acad Sci U S A* 2006;**103**:15497−501.
16. Li Q, Chen J, Xiao Y, Di P, Zhang L, Chen W. The dirigent multigene family in Isatis indigotica: gene discovery and differential transcript abundance. *BMC Genom* 2014;**15**:388.
17. Chen R, Li Q, Tan H, Chen J, Xiao Y, Ma R, et al. Gene-to-metabolite network for biosynthesis of lignans in MeJA-elicited Isatis indigotica hairy root cultures. *Front Plant Sci* 2015;**6**:952.
18. Wang S, Wu C, Li X, Zhou Y, Zhang Q, Ma F, et al. Syringaresinol-4-*O*-beta-D-glucoside alters lipid and glucose metabolism in HepG2 cells and C2C12 myotubes. *Acta Pharm Sin B* 2017;**7**:453−60.
19. Zhang Y, Lv X, Qu J, Zhang X, Zhang M, Gao H, et al. A systematic strategy for screening therapeutic constituents of *Schisandra chinensis* (Turcz.) Baill infiltrated blood-brain barrier oriented in lesions using ethanol and water extracts: a novel perspective for exploring chemical material basis of herb medicines. *Acta Pharm Sin B* 2020;**10**:557−68.
20. Nakai M, Harada M, Nakahara K, Akimoto K, Shibata H, Miki W, et al. Novel antioxidative metabolites in rat liver with ingested sesamin. *J Agric Food Chem* 2003;**51**:1666−70.
21. Mottaghi S, Abbaszadeh H. A comprehensive mechanistic insight into the dietary and estrogenic lignans, arctigenin and sesamin as potential anticarcinogenic and anticancer agents. Current status, challenges, and future perspectives. *Crit Rev Food Sci Nutr* 2022;**62**:7301−18.
22. Majdalawieh AF, Yousef SM, Abu-Yousef IA, Nasrallah GK. Immunomodulatory and anti-inflammatory effects of sesamin: mechanisms of action and future directions. *Crit Rev Food Sci Nutr* 2022;**62**:5081−112.
23. Zhao W, Cong Y, Li HM, Li S, Shen Y, Qi Q, et al. Challenges and potential for improving the druggability of podophyllotoxin-derived drugs in cancer chemotherapy. *Nat Prod Rep* 2021;**38**:470−88.
24. Lin JL, Fang X, Li JX, Chen ZW, Wu WK, Guo XX, et al. Dirigent gene editing of gossypol enantiomers for toxicity-depleted cotton seeds. *Nat Plants* 2023;**9**:605−15.
25. Li J, Zhou B, Li C, Chen Q, Wang Y, Li Z, et al. Lariciresinol-4-*O*-beta-D-glucopyranoside from the root of Isatis indigotica inhibits influenza A virus-induced pro-inflammatory response. *J Ethnopharmacol* 2015;**174**:379−86.
26. Yang Z, Wang Y, Zheng Z, Zhao S, Zhao J, Lin Q, et al. Antiviral activity of *Isatis indigotica* root-derived clemastanin B against human and avian influenza A and B viruses *in vitro*. *Int J Mol Med* 2013;**31**:867−73.

27. Xiao Y, Shao K, Zhou J, Wang L, Ma X, Wu D, et al. Structure-based engineering of substrate specificity for pinoresinol-lariciresinol reductases. *Nat Commun* 2021;**12**:2828.
28. Xiao Y, Ji Q, Gao S, Tan H, Chen R, Li Q, et al. Combined transcriptome and metabolite profiling reveals that *Ii*PLR1 plays an important role in lariciresinol accumulation in *Isatis indigotica*. *J Exp Bot* 2015;**66**:6259−71.
29. Chen X, Chen J, Feng J, Wang Y, Li S, Xiao Y, et al. Tandem UGT71B5s catalyze lignan glycosylation in *Isatis indigotica* with substrates promiscuity. *Front Plant Sci* 2021;**12**:637695.
30. Tan Y, Yang J, Jiang Y, Wang J, Liu Y, Zhao Y, et al. Functional characterization of UDP-glycosyltransferases involved in anti-viral lignan glycosides biosynthesis in *Isatis indigotic*a. *Front Plant Sci* 2022;**13**:921815.
31. Wang X, Wang S, Lin Q, Lu J, Lv S, Zhang Y, et al. The wild allotetraploid sesame genome provides novel insights into evolution and lignan biosynthesis. *J Adv Res* 2022;**1232**:233−8.
32. Pickel B, Constantin MA, Pfannstiel J, Conrad J, Beifuss U, Schaller A. An enantiocomplementary dirigent protein for the enantioselective laccase-catalyzed oxidative coupling of phenols. *Angew Chem Int Ed Engl* 2010;**49**:202−4.
33. Davin LB, Wang HB, Crowell AL, Bedgar DL, Martin DM, Sarkanen S, et al. Stereoselective bimolecular phenoxy radical coupling by an auxiliary (dirigent) protein without an active center. *Science* 1997;**275**:362−6.
34. Hosmani PS, Kamiya T, Danku J, Naseer S, Geldner N, Guerinot ML, et al. Dirigent domain-containing protein is part of the machinery required for formation of the lignin-based Casparian strip in the root. *Proc Natl Acad Sci U S A* 2013;**110**:14498−503.
35. Effenberger I, Harport M, Pfannstiel J, Klaiber I, Schaller A. Expression in *Pichia pastoris* and characterization of two novel dirigent proteins for atropselective formation of gossypol. *Appl Microbiol Biotechnol* 2017;**101**:2021−32.
36. Effenberger I, Zhang B, Li L, Wang Q, Liu Y, Klaiber I, et al. Dirigent proteins from cotton (*Gossypium* sp.) for the atropselective synthesis of gossypol. *Angew Chem Int Ed Engl* 2015;**54**:14660−3.
37. Li L, Sun W, Wang P, Li H, Rehman S, Li D, et al. Characterization, expression, and functional analysis of the pathogenesis-related gene *Pt*DIR11 in transgenic poplar. *Int J Biol Macromol* 2022;**210**:182−95.
38. Zhang L, Chen J, Zhou X, Chen X, Li Q, Tan H, et al. Dynamic metabolic and transcriptomic profiling of methyl jasmonate-treated hairy roots reveals synthetic characters and regulators of lignan biosynthesis in *Isatis indigotica* Fort. *Plant Biotechnol J* 2016;**14**:2217−27.
39. Chen J, Dong X, Li Q, Zhou X, Gao S, Chen R, et al. Biosynthesis of the active compounds of *Isatis indigotica* based on transcriptome sequencing and metabolites profiling. *BMC Genom* 2013;**14**:857.
40. Xiao Y, Feng J, Li Q, Zhou Y, Bu Q, Zhou J, et al. *Ii*WRKY34 positively regulates yield, lignan biosynthesis and stress tolerance in *Isatis indigotica*. *Acta Pharm Sin B* 2020;**10**:2417−32.
41. Ma R, Xiao Y, Lv Z, Tan H, Chen R, Li Q, et al. AP2/ERF transcription factor, *Ii*049, positively regulates lignan biosynthesis in *Isatis indigotica* through activating salicylic acid signaling and lignan/lignin pathway genes. *Front Plant Sci* 2017;**8**:1361.
42. Meng L, Guo Q, Liu Y, Shi J. 8,4′-Oxyneolignane glucosides from an aqueous extract of "ban lan gen" (*Isatis indigotica* root) and their absolute configurations. *Acta Pharm Sin B* 2017;**7**:638−46.
43. Guo Q, Li D, Xu C, Zhu C, Guo Y, Yu H, et al. Indole alkaloid glycosides with a 1′-(phenyl)ethyl unit from *Isatis indigotica* leaves. *Acta Pharm Sin B* 2020;**10**:895−902.
44. Zhou Z, Tan H, Li Q, Chen J, Gao S, Wang Y, et al. CRISPR/Cas9-mediated efficient targeted mutagenesis of RAS in *Salvia miltiorrhiza*. *Phytochemistry* 2018;**148**:63−70.
45. Zhang Z, Mao Y, Ha S, Liu W, Botella JR, Zhu JK. A multiplex CRISPR/Cas9 platform for fast and efficient editing of multiple genes in *Arabidopsis*. *Plant Cell Rep* 2016;**35**:1519−33.
46. Kazenwadel C, Klebensberger J, Richter S, Pfannstiel J, Gerken U, Pickel B, et al. Optimized expression of the dirigent protein *At*DIR6 in *Pichia pastoris* and impact of glycosylation on protein structure and function. *Appl Microbiol Biotechnol* 2013;**97**:7215−27.
47. Chen J, Wang Y, Liang F, Zhou X, Chen X, Lu M, et al. *Ii*UGT71B2 catalyzes lignan glycosylation in *Isatis indigotica* with substrates specificity. *Ind Crop Prod* 2023;**195**:116483.
48. Chen C, Chen H, Zhang Y, Thomas HR, Frank MH, He Y, et al. TBtools: an integrative toolkit developed for interactive analyses of big biological data. *Mol Plant* 2020;**13**:1194−202.
49. Ralph SG, Jancsik S, Bohlmann J. Dirigent proteins in conifer defense II: extended gene discovery, phylogeny, and constitutive and stress-induced gene expression in spruce (Picea spp.). *Phytochemistry* 2007;**68**:1975−91.
50. Kim KW, Moinuddin SG, Atwell KM, Costa MA, Davin LB, Lewis NG. Opposite stereoselectivities of dirigent proteins in *Arabidopsis* and schizandra species. *J Biol Chem* 2012;**287**:33957−72.
51. Halls SC, Davin LB, Kramer DM, Lewis NG. Kinetic study of coniferyl alcohol radical binding to the (+)-pinoresinol forming dirigent protein. *Biochemistry* 2004;**43**:2587−95.
52. Hou M, Wang R, Zhao S, Wang Z. Ginsenosides in *Panax genus* and their biosynthesis. *Acta Pharm Sin B* 2021;**11**:1813−34.
53. Yin Y, Li Y, Jiang D, Zhang X, Gao W, Liu C. *De novo* biosynthesis of liquiritin in *Saccharomyces cerevisiae*. *Acta Pharm Sin B* 2020;**10**:711−21.
54. Tan Y, Yang J, Jiang Y, Sun S, Wei X, Wang R, et al. Identification and characterization of two *Isatis indigotica O*-methyltransferases methylating *C*-glycosylflavonoids. *Hortic Res* 2022;**9**:140.
55. Paniagua C, Bilkova A, Jackson P, Dabravolski S, Riber W, Didi V, et al. Dirigent proteins in plants: modulating cell wall metabolism during abiotic and biotic stress exposure. *J Exp Bot* 2017;**68**:3287−301.
56. Guo JL, Xu LP, Fang JP, Su YC, Fu HY, Que YX, et al. A novel dirigent protein gene with highly stem-specific expression from sugarcane, response to drought, salt and oxidative stresses. *Plant Cell Rep* 2012;**31**:1801−12.
57. Ralph S, Park JY, Bohlmann J, Mansfield SD. Dirigent proteins in conifer defense: gene discovery, phylogeny, and differential wound- and insect-induced expression of a family of DIR and DIR-like genes in spruce (Picea spp.). *Plant Mol Biol* 2006;**60**:21−40.
58. Karlova R, Boer D, Hayes S, Testerink C. Root plasticity under abiotic stress. *Plant Physiol* 2021;**187**:1057−70.
59. Huang J, Zhao X, Burger M, Wang Y, Chory J. Two interacting ethylene response factors regulate heat stress response. *Plant Cell* 2021;**33**:338−57.
60. Licausi F, Ohme-Takagi M, Perata P. APETALA2/Ethylene Responsive Factor (AP2/ERF) transcription factors: mediators of stress responses and developmental programs. *New Phytol* 2013;**199**:639−49.
61. Schmidt R, Mieulet D, Hubberten HM, Obata T, Hoefgen R, Fernie AR, et al. Salt-responsive ERF1 regulates reactive oxygen species-dependent signaling during the initial response to salt stress in rice. *Plant Cell* 2013;**25**:2115−31.
62. Cheng MC, Liao PM, Kuo WW, Lin TP. The Arabidopsis ETHYLENE RESPONSE FACTOR1 regulates abiotic stress-responsive gene expression by binding to different *cis*-acting elements in response to different stress signals. *Plant Physiol* 2013;**162**:1566−82.
63. Anderson JP, Badruzsaufari E, Schenk PM, Manners JM, Desmond OJ, Ehlert C, et al. Antagonistic interaction between abscisic acid and jasmonate-ethylene signaling pathways modulates defense gene expression and disease resistance in Arabidopsis. *Plant Cell* 2004;**16**:3460−79.
64. Waadt R, Seller CA, Hsu PK, Takahashi Y, Munemasa S, Schroeder JI. Plant hormone regulation of abiotic stress responses. *Nat Rev Mol Cell Biol* 2022;**23**:680−94.
65. Ma X, Chen L, Zhu Q, Chen Y, Liu YG. Rapid decoding of sequence-specific nuclease-induced heterozygous and biallelic mutations by direct sequencing of PCR products. *Mol Plant* 2015;**8**:1285−7.

66. Muthuramalingam M, Zeng X, Iyer NJ, Klein P, Mahalingam R. A GCC-box motif in the promoter of nudix hydrolase 7 (*At*NUDT7) gene plays a role in ozone response of *Arabidopsis* ecotypes. *Genomics* 2015;**105**:31−8.
67. Schmidt R, Schippers JH, Mieulet D, Watanabe M, Hoefgen R, Guiderdoni E, et al. Salt-responsive ERF1 is a negative regulator of grain filling and gibberellin-mediated seedling establishment in rice. *Mol Plant* 2014;**7**:404−21.
68. Li Y, Zhou J, Li Z, Qiao J, Quan R, Wang J, et al. Salt and aba response ERF1 improves seed germination and salt tolerance by repressing ABA signaling in rice. *Plant Physiol* 2022;**189**:1110−27.
69. Yu ZX, Li JX, Yang CQ, Hu WL, Wang LJ, Chen XY. The jasmonate-responsive AP2/ERF transcription factors *Aa*ERF1 and *Aa*ERF2 positively regulate artemisinin biosynthesis in *Artemisia annua* L. *Mol Plant* 2012;**5**:353−65.
70. Cheong JJ, Choi YD. Methyl jasmonate as a vital substance in plants. *Trends Genet* 2003;**19**:409−13.
71. Wang Y, Mostafa S, Zeng W, Jin B. Function and mechanism of jasmonic acid in plant responses to abiotic and biotic stresses. *Int J Mol Sci* 2021;**22**:8568.
72. Davin LB, Jourdes M, Patten AM, Kim KW, Vassao DG, Lewis NG. Dissection of lignin macromolecular configuration and assembly: comparison to related biochemical processes in allyl/propenyl phenol and lignan biosynthesis. *Nat Prod Rep* 2008;**25**:1015−90.
73. Dalisay DS, Kim KW, Lee C, Yang H, Rubel O, Bowen BP, et al. Dirigent protein-mediated lignan and cyanogenic glucoside formation in flax seed: integrated omics and maldi mass spectrometry imaging. *J Nat Prod* 2015;**78**:1231−42.
74. Gasper R, Effenberger I, Kolesinski P, Terlecka B, Hofmann E, Schaller A. Dirigent protein mode of action revealed by the crystal structure of *At*DIR6. *Plant Physiol* 2016;**172**:2165−75.
75. Kim MK, Jeon JH, Fujita M, Davin LB, Lewis NG. The western red cedar (*Thuja plicata*) 8-8′ DIRIGENT family displays diverse expression patterns and conserved monolignol coupling specificity. *Plant Mol Biol* 2002;**49**:199−214.
76. Qi J, Song CP, Wang B, Zhou J, Kangasjarvi J, Zhu JK, et al. Reactive oxygen species signaling and stomatal movement in plant responses to drought stress and pathogen attack. *J Integr Plant Biol* 2018;**60**:805−26.
77. Zhang Y, Zhao H, Di Y, Qi L, Shao D, Shi J, et al. Antitumor activity of pinoresinol *in vitro*: inducing apoptosis and inhibiting HepG2 invasion. *J Funct Foods* 2018;**45**:206−14.
78. Sepporta MV, Mazza T, Morozzi G, Fabiani R. Pinoresinol inhibits proliferation and induces differentiation on human HL60 leukemia cells. *Nutr Cancer* 2013;**65**:1208−18.
79. Horwitz C, Rozen P. Lignans and phytoestrogens. *Front Gastrointest Res* 1988;**14**:165−76.
80. Thompson LU, Orcheson L, Richard S, Jenab M, Serraino M, Seidl M, et al. Anticancer effects of flaxseed lignans. In: Kumpulainen JT, Salonen JT, editors. *Natural antioxidants and food quality in atherosclerosis and cancer prevention*. Cambridge: Woodhead Publishing; 1996. p. 356−64.
81. Greco FA, Thompson DS, Morrissey LH, Erland JB, Burris 3rd HA, Spigel DR, et al. Paclitaxel/carboplatin/etoposide versus paclitaxel/topotecan for extensive-stage small cell lung cancer: a minnie pearl cancer research network randomized, prospective phase II trial. *Oncol* 2005;**10**:728−33.
82. Kopp HG, Kuczyk M, Classen J, Stenzl A, Kanz L, Mayer F, et al. Advances in the treatment of testicular cancer. *Drugs* 2006;**66**:641−59.
83. Hande KR. Etoposide: four decades of development of a topoisomerase II inhibitor. *Eur J Cancer* 1998;**34**:1514−21.